Numerical Analysis of Train-Induced Vibrations Effect on Existing Masonry Building

Qian Xia, Wen-Jun Qu, Yi-Qing Li, Jin Zhao and Meng-Yun Gan

Abstract Based on the masonry structures in Shanghai adjacent to the subway, this paper sets up a detailed numerical model. Measured vibration acceleration serves as the input excitation, and the parameters of the model were calibrated by the measured vibration response. Through numerical analysis, it is studied that metro train-induced vibrations and their influences on existing masonry building from two aspects—one is the vibration level changing with the story height, and the other is the vibration level changing at all the rooms on one floor—the different slab properties, different room size, and other factors affected vibration response distribution. In the precast slab room, the vertical vibration arrangement is greater than that in the cast in situ floor slab room. Vertical vibration at the ash between the precast slabs had a certain amplification effect; the room depth parameters had a small effect on the vibration intensity. The width of the room has a significant effect on the vertical vibration.

Keywords Subway-induced vibration · Masonry building · Numerical analysis · Vibration distribution characteristics · Slab properties

Q. Xia (✉)
School of Civil Engineering and Architecture, Xi'an University of Technology, Xi'an 710048, China
e-mail: ice69pipiniu@163.com

W.-J. Qu
College of Civil Engineering, Tongji University, Shanghai 200092, China
e-mail: quwenjun.tj@tongji.edu.cn

Y.-Q. Li · J. Zhao
Shaanxi Jianda Weigu Quality Testing Technology Co. Ltd, Xi'an 710055, China
e-mail: liyiqing1984@163.com

J. Zhao
e-mail: zhaojin13335@163.com

M.-Y. Gan
School of Civil Engineering, Tianjin University, Tianjin 300350, China
e-mail: gmy_why@163.com

E. Tutumluer et al. (eds.), *Advances in Environmental Vibration and Transportation Geodynamics*, Lecture Notes in Civil Engineering 66,
https://doi.org/10.1007/978-981-15-2349-6_6

1 Instructions

The urban transportation route selected for this study is based on its forecast on the volume of travelers; the route does not avoid densely populated areas, the safety of sensitive, and demand for special functions that are affected by long-term vibration. In recent years, studies both local and international on free-field ground motion regularity caused by the subway have been unrestricted. Research on special sensitive construction affected by the vibration was mainly focused on the forecasting methods and the evaluation of the case [1]. Subjects of the studies include bank buildings [2, 3], scientific research institutes [4, 5], places of historic interest [6, 7], and museums [1]. The varied materials and the construction form of these buildings introduce difficulties to the study of the vibration distribution.

Masonry structure, compared with the different construction forms of tall steel structures, such as steel and concrete composite structure, has a single architectural form. Its structure is usually the same as the surrounding buildings in the area, with the same materials, number of layers, scale, and shape. As such, the study of its corresponding vibration distribution is convenient. In this paper, the background of the old city in Shanghai is presented, in which its existing masonry buildings are influenced by the subway. By integrating two residential projects in Shanghai, this paper will discuss the field testing of the three directions of vibration on one vertical and two horizontal directions, i.e., the *X*-, *Y*-axes of the masonry buildings resulting from the subway movement. A numerical model for the two residential buildings is also presented showing the collection of real information of the two buildings. Thereafter, an analysis and comparison of the results from two different methods which are field-measured data and numerical analysis model vibration data will be discussed. Beyond presenting the principles of the vibration system of the masonry structure, this paper will also provide valid data to guide future research.

This paper combines the numerical simulation and testing method to study the existing masonry structure in a vibration environment caused by the urban rail movement. This will address the environmental vibration problems in this aspect.

2 Experimental Introduction

The test site is located by the subway line of a station in Shanghai. The test field includes two ordinary brick residential buildings close to metro line one (Fig. 1).

The test residential buildings were built in the 1960s. The two buildings are a five-story brick and concrete, rectangular structure. Building 1 has an east–west length at 28.8 m, with its north–south dimensions approximately 12.1 m wide, with a construction area of approximately 1742 m^2; Building 2 has an east-west length of 22.5 m, with a north–south width of approximately 12 m. The first and second buildings' distances from the centerline of the orbit are 22 m and 10 m, respectively. The structures are horizontal load-bearing wall systems with no basements. And the floor spacing 2.8 m on each floor is a precast slab.

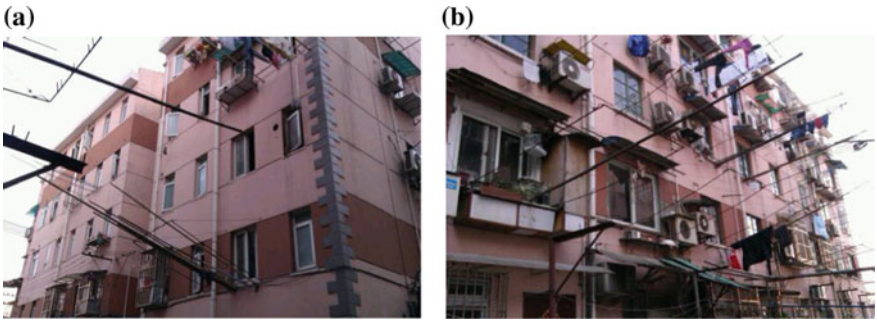

Fig. 1 Test building photographs: **a** north elevation, **b** south elevation

The sensor arrangement of the building is shown in Fig. 2. The B-D axis of Building 1 and Building 2 is a stairwell with a span of 1.35 m. The two spans of B-D and D-E in Building 1 and Building 2 are both indoor rooms. The span of the slab is 4.8 m and 5.2 m, respectively. In order to compare the vibrations in the three directions of the slab, sensors are installed in the stairwells on the first, third, and fifth floors of Building 1 and Building 2 and the indoor floor on the second and fourth floors. In order to compare the vibration of the floor slab, a second placement scheme was made for Building 2, and a sensor was placed on each floor of the stairwell to test the vertical direction (*Z*-direction) and horizontal direction (*X*-direction along the longitudinal direction of the building and *Y*-direction along the lateral direction of the building). Because of the limited number of sensors, the vertical and horizontal vibrations of buildings are tested in groups.

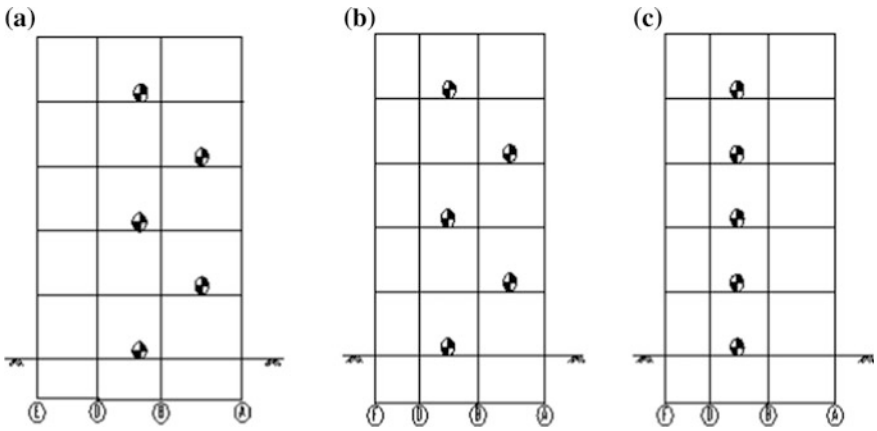

Fig. 2 Layout of measuring points on buildings: **a** in Building 1, **b** plan 1 for Building 2, **c** plan 2 for Building 2

3 Numerical Analysis of Masonry Building

Several factors such as vibration source, propagation path, and building structure influence the metro-induced vibration of the buildings. All subsystems considered during numerical modeling can cause complications and result in inaccurate predictions. The three-dimensional finite element model of the masonry structure is set up in this paper, using the measurements of the part of the room to adjust model parameters, and the adjusted model is applied to the analysis of the vibration distribution of each room in the entire building.

3.1 The Research Object and Size of the Model

The simulation study is based on Building 2 as the research object; the building's distance from the centerline of the orbit is 10 m. The model in this article is set up based on the actual situation of the masonry structure. In order to simulate the vibration of real masonry structure as far as possible, the numerical model is established by ANSYS finite element software according to the actual situation of masonry structure including staircase (Fig. 3).

3.2 Unit Type and Component Section

The floor and wall of the building are simulated by SHELL181, and the beam and column are made of BEAM188. The thickness of the brick wall is 240 mm; the single-layer SHELL element is used to give masonry material property. The thickness of prestressed hollow slabs is 100 mm, and that of some cast-in-place slabs is 100 mm, to give concrete properties. It is worth knowing that, because of the plastering gap connection between the precast slabs, the strength of the plastering gap is much lower than that of the precast slab; it can be neglected, that is, when the model is established, the plastering gap edge of the precast slab connection is

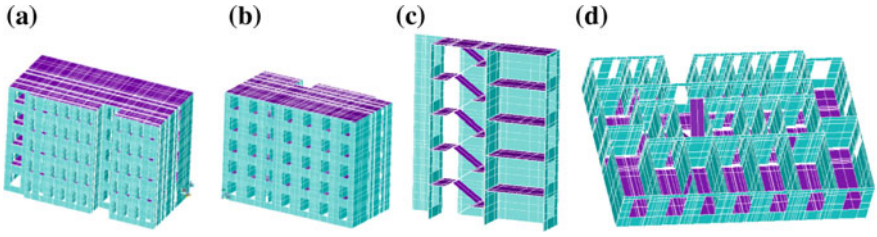

Fig. 3 Sketch map of the finite element model: **a** north elevation, **b** south elevation, **c** profile map of the staircase, **d** plane graph

considered by the free side. However, because of the huge memory occupied by the building 3D numerical model and the limited computing ability of the computer, it is not possible to make the simulation of the plastering gap between the various precast slabs. Therefore, the author only makes the plastering gap treatment on the wall edge position of the precast slab layout direction, that is, the precast slab boundary is made into a free edge. The sections of beams and columns are user-defined, and longitudinal steel bars are arranged at four corners. As shown in Figs. 4 and 5, the section of the ring beam is 240 × 240, the section of the staircase beam is 240 × 300, and the section of the column is 240 × 240. With the same reinforcement at the bottom and top of the section of the ring beam and the structural column, the longitudinal reinforcement area is $A_s = 24 \times 24 \times 2 = 1152\,\text{mm}^2$. The ratio of reinforcement at the bottom and top of the section is 2.0%.

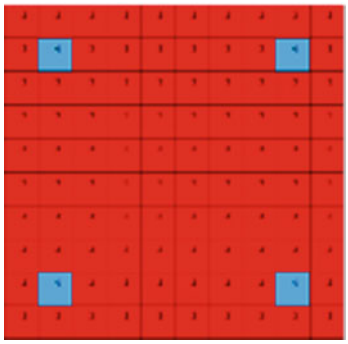

Fig. 4 Section of a ring beam

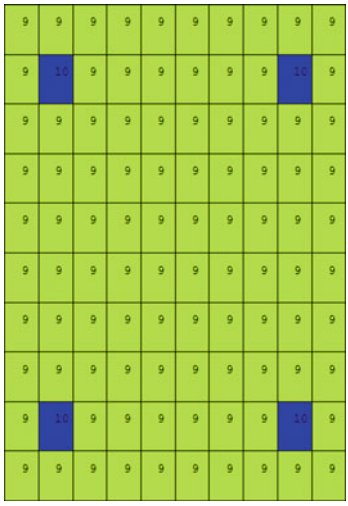

Fig. 5 Section of a structural column

3.3 Material Properties and the Selection of the Model Size

The material data collected on the spot are limited, so it is only for reference. In the program, the strength grade of sintered ordinary brick is MU10, mortar strength grade is M2.5, and the design value of compressive strength of sintered ordinary brick masonry is 1.30 MPa. It is considered that the quality control grade of masonry construction can reach the B level specified in <Code for acceptance of construction quality of masonry engineering> (GB 50203-2002) [8] and take the partial coefficient of material properties $\gamma_f = 1.6$.

$$f_k = \gamma_f \times f = 1.6 \times 1.30 = 2.08\,\text{MPa} \tag{1}$$

According to <Unified standard for reliability design of building structures> GB 50068 [9], the relationship between the standard value of masonry strength and the average value is

$$f_k = f_m(1 - 1.645\delta_f). \tag{2}$$

In the formula: f_k—standard value of masonry strength;

δ_f—the coefficient of variation of masonry strength, that is determined by statistics of test results.

According to the description of provisions of <Code for design of masonry structures> (GB 50003-2001), the coefficient of variation in the formula of the average strength of sintered ordinary brick masonry is $\delta_f = 0.205$. The masonry structure studied in this paper was constructed between 1985 and 1994 and, therefore, takes a low coefficient of variation $\delta_f = 0.1$. So the average value of masonry strength is:

$$f_m = \frac{f_k}{(1 - 1.645\delta_f)} = \frac{2.08}{(1 - 1.645 \times 0.1)}\,\text{MPa} \approx 2.5\,\text{MPa} \tag{3}$$

The strength grade of concrete is C20, the design value of the compressive strength f_c is 9.6 MPa, the average value of the compressive strength of the masonry f_m is 2.5 MPa, the strength classes of steel bar are HRB335, and the design value of the yield strength f_y is 300 MPa. The material properties are shown in Table 1.

Table 1 Material properties

Properties	Initial elastic modulus (MPa)	Poisson ratio	Density (kg/m^3)	Damping ratio	Intensity (MPa)
Concrete	0.912×10^4	0.2	2500	0.1	9.6
Masonry	0.1553×10^4	0.16	1800	0.07	2.5
Steel bar	2.1×10^5	0.3	7850	–	300

The mathematical expression of stress–strain relation of concrete under axial compression proposed by <Code for design of concrete structures> (GB 50010) [10] is as follows:

$$\left.\begin{array}{ll}\sigma_c = f_c\left[1-\left(1-\frac{\varepsilon_c}{\varepsilon_0}\right)^n\right] & \varepsilon_c \le \varepsilon_0 \\ \sigma_c = f_c & \varepsilon_0 < \varepsilon_c \le \varepsilon_{cu}\end{array}\right\} \tag{4}$$

$$n = 2 - \frac{1}{60}(f_{cu} - 50) \tag{5}$$

$$\begin{aligned}\varepsilon_0 &= 0.002 + 0.5(f_{cu} - 50) \times 10^{-5} \\ \varepsilon_u &= 0.0033 - (f_{cu} - 50) \times 10^{-5}.\end{aligned} \tag{6}$$

The stress–strain relationship of masonry materials under compression is shown in Fig. 6.

The vibration of the subway studied in this paper belongs to elastic deformation, so the stress–strain curves of masonry at f_m = 2.5 MPa are shown in Fig. 7.

In order to simulate the subway environment vibration performance of the real structure, and based on the past studies [11], the present study has chosen the concrete damping ratio at 10% and the masonry material damping ratio at 7%.

In analyzing the unit division of the structure, considering the small speed of the bending wave, and following 1/8 of the fluctuation refining standard, the unit division of the beam, the column, and the slab, the maximum size of the unit is mainly affected by the beam height and the slab thickness. The largest unit size is 0.5 m when the vibration frequency is 80 Hz. The accuracy of the calculation is ensured following the size of this division.

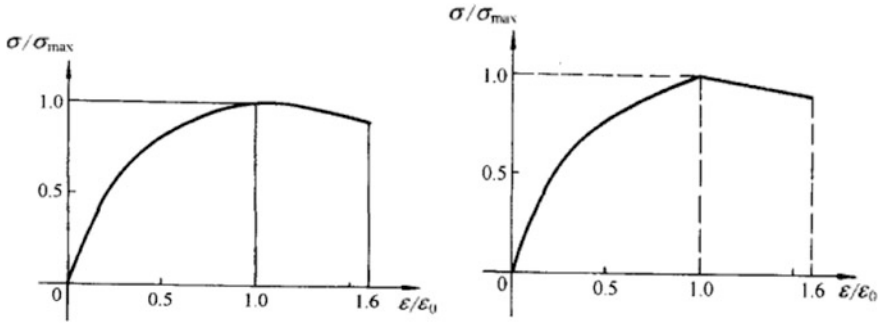

Fig. 6 Compressive stress–strain curve of masonry

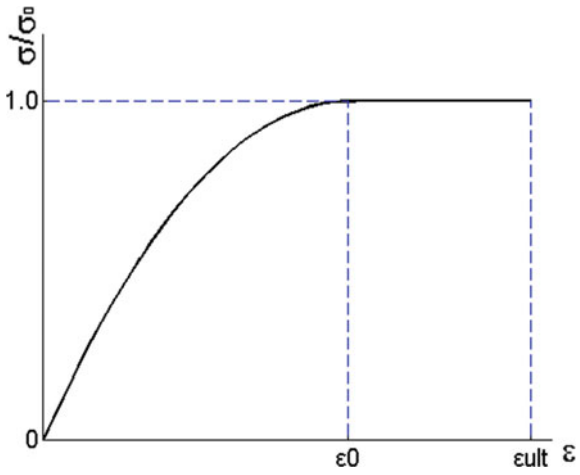

Fig. 7 Compressive stress–strain curve of masonry used in this paper (using elastic section)

3.4 Incentive Load Input

In order to analyze the vibration response discipline, the interaction between the soil and the structure is disregarded, and the relative motion method is used. Past studies [12] recommend that under the vibration environment, the building's vibration may be calculated regardless of the interaction between the soil and the structure. The building's bottom input data consider the measured acceleration time history in the wall–floor junction and input the data based on the consistent incentive method (Fig. 8). Studies [13, 14] also recommend the safety of this method. Using Rayleigh damping, with the building fundamental frequency and 80 Hz, the system damping ratio is 0.05, thus obtaining the Rayleigh damping coefficient. The Newmark direct integral method is adopted from dynamic analysis, and the time step is 0.005 s.

It can be observed from Fig. 8 that the duration of the influence of the subway train on the vibration of the building is about 10 s. In the frequency spectrum, the vibration has a peak value in both 0–20 and 40–70 Hz, and the peak value of 40–70 Hz is larger.

4 Model Checking

4.1 Vertical Vibration Level Analysis Comparison

The vertical acceleration at indoor rooms on floors 2, 4 and in the staircase on floors 3, 5 is used to check the model. Details for each room are shown in Fig. 9.

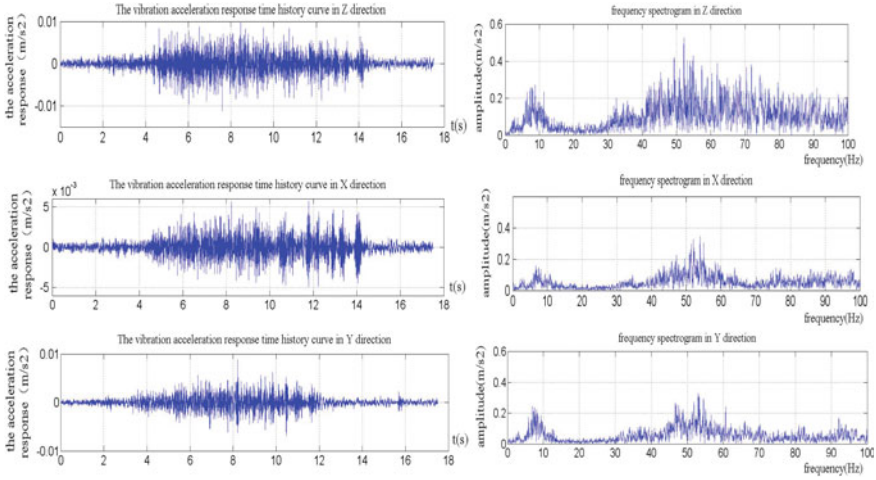

Fig. 8 Time history and Fourier spectrum of input accelerations

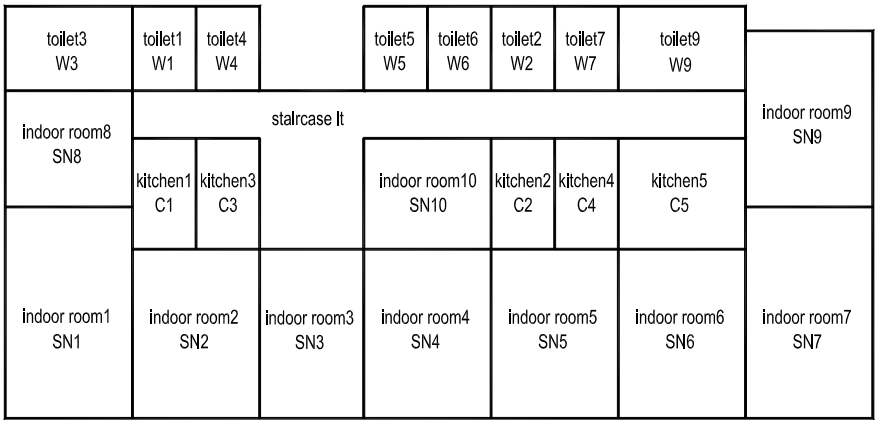

Fig. 9 Interior room details

Figure 10 shows the change curve with the changing stories of the calculated and the measured values of Z vibration level. The changes in rules and values are consistent, and the maximum deviation is 1.4 dB (Table 2).

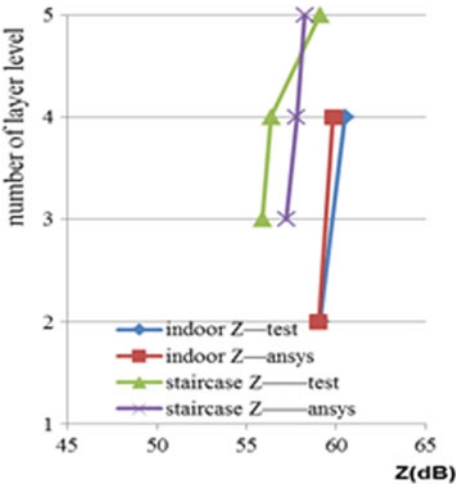

Fig. 10 Comparison of calculated and measured vertical vibration level

Table 2 Calculation error of vertical vibration level

Maximum deviation	Indoor room	Staircase
2nd floor	−0.1	–
3rd floor	–	1.3
4th floor	−0.7	1.4
5th floor	–	−0.8

Negative values represent the model vibration results less than the test vibration results

4.2 Vibration Acceleration Level Comparison

As a further contrast of vibration response in different positions on one floor in the one-third octave band domain, only vertical acceleration level of the fourth floor is shown because of the limited length (Fig. 11). The visible contrast corresponds with the calculated value in each center frequency.

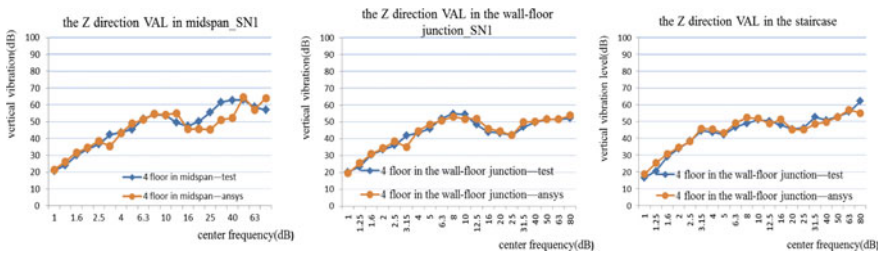

Fig. 11 Comparison of calculated and measured acceleration level in a vertical direction

5 Analysis of Vibration Response Regularity

In order to compensate for the limitations of the test, the model was checked and the vibration response regularity was further analyzed in different rooms.

5.1 Changes in Vibration Along Floor Heights

Comparison of Vibration Between the Mid-span and the Wall–Floor Junction Contrasting the vertical vibration between the mid-span and the wall–floor junction, with the subway passing the structure, the rooms SN2, C1, C2, W1, and W2 were taken as examples. Figure 12 lists only the vibration of the two floors (the second and fifth floors) because of limited length. The results show that when the subway passed, the vertical vibration at larger mid-spans was 1–3 dB higher than that at the junction. The vertical vibration in smaller rooms such as the kitchen or restroom was 0.3–2 dB higher than that in the wall–floor junction. The vibration response in all rooms indicates that the vibration level on the fifth floor is higher than that on the second floor at the mid-span and the wall–floor junction.

Comparison of Vibrations Between the Precast Slab Room and the Cast In Situ Floor Slab Room This study aims to examine the existing masonry structure of environmental vibration and floor characteristics. The two kinds of slab features are the precast slab and the cast in situ floor slab. In the actual structure, the majority of older buildings use precast slab, and only certain portions of the building use the cast in situ slab, following the building function. This situation is a common practice. The two buildings in the experiment belong to this type. A numerical model was set up close to the actual situation, as well as the establishment of the precast slab and cast in situ floor slab. These are essential for the analysis of the floor characteristics.

In the test building, with the need for function, the bathroom floor uses the cast in situ floor slab and the rest of the room use cheap precast slab. In order to avoid other factors on the characteristics of the floor in the research on the effects of

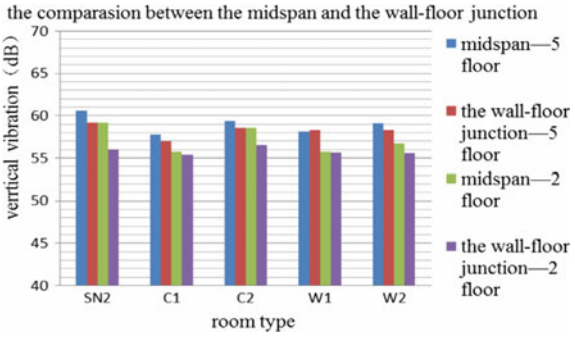

Fig. 12 Vibration response comparison on the 2nd and 5th floor at mid-span and the wall–floor junction

vibration, almost the same kitchen of other parameters was chosen, compared with the vibration of the position corresponding to the toilet. Figure 13 shows the comparison of the C1 and W1, and C2 and W2; it can be seen, in every floor, vertical vibration level: Vibration strength of C1 and W1 generally is consistent, and vertical vibration of C2 is higher than the vibration of the W2 about 3–3.5 dB. Overall, the cheap precast slab has a certain extent amplification effect of vertical vibration, while the cast in situ floor slab has a relative attenuation effect of vertical vibration; the reason should be its material properties.

Precast slab ash seam position (arrow position) vibration intensity compared with no mortar joint processing of the precast slab vibration intensity is high about 2–3 dB; it is visible of the vibration strength amplification between the precast slabs of ash seam, and the magnifying effect cannot be ignored. From the point of view about the simplified model, mortar joint treatment only sets up at the corner of the wall along the precast slab layout direction. The actual situation, that is, the mortar joint is built between each precast slab, further infers that vertical vibration strength of the precast slab room is greater than that in the cast in situ floor slab room (Fig. 14) [15, 16].

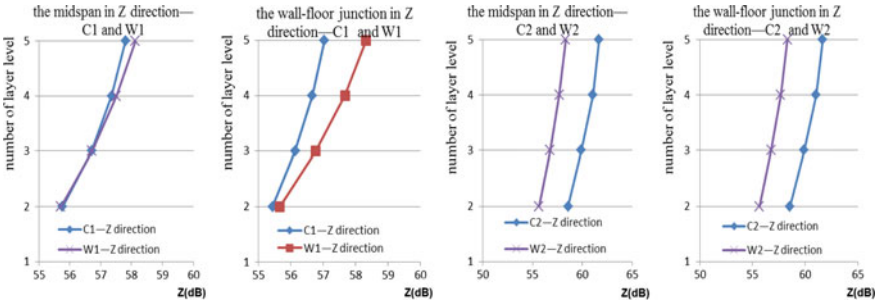

Fig. 13 Comparison of vibration level in the vertical directions at mid-span and the wall–floor junction with the story height between the kitchen room and washroom

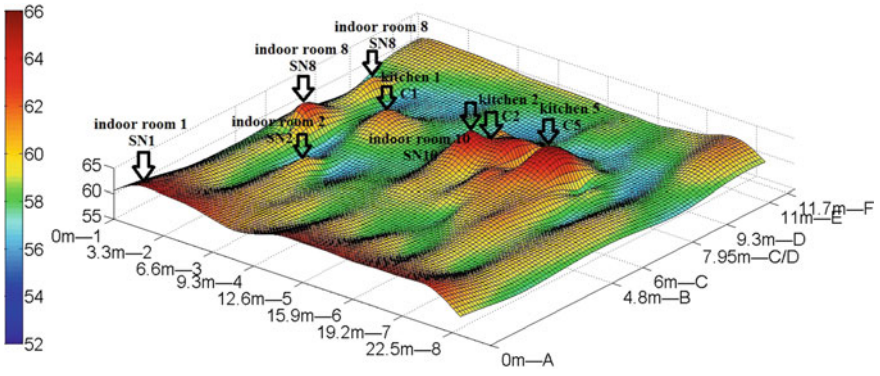

Fig. 14 Three-dimensional images of vertical vibration at all rooms on one floor

Impact of Width and Depth of the Room and the Wall Constraint Condition on Vibration In order to study the parameter about the depth of the room influence on the vibration, this paper chose the SN1 and SN2 in which the depth of the room is different, while the other parameters are almost the same and compare the vibration of these two rooms. The width of the two rooms is all 3.3 m, and the depth of the two rooms is 6 m and 4.8 m, respectively (Fig. 15). In addition to the same vibration strength in the *Y*-direction on 3 and 4 floors, the vibration strength in three directions on each floor is that in SN2 it is greater than that in SN1. The maximum deviation is only 0.2 dB; the depth of the room influence on the vibration strength is small and negligible.

In order to study the influence of room width on vibration, C1 and C5 were selected. The room widths are different, whereas the other parameters and the constraint condition are almost the same. Thus, the vibration of C1 and C5 is compared. The rooms both have depths of 3.15 m, and the widths of C1 and C5 are 1.65 m and 3.3 m, respectively. The results are shown in Fig. 16. The comparison of vibration level in the three directions obtained from the two rooms indicates that the horizontal vibration intensity is almost the same, and the vertical vibration in C5 is greater than that in C1. The maximum deviation is only 3.6 dB on the top of the floor; the width of the room has no significant effect on horizontal vibration and greatly affects vertical vibration. The large width of the room corresponds to great vibration intensity.

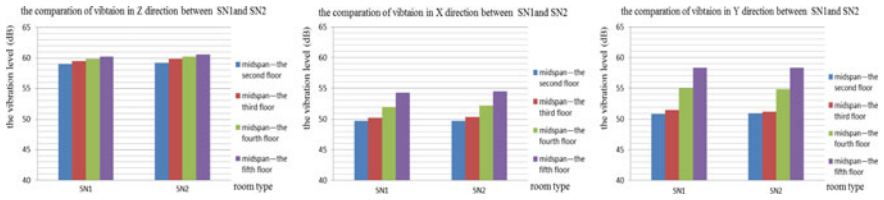

Fig. 15 Comparison of vibration level in the three directions in the mid-span floor along the floor height between the SN1 and SN2

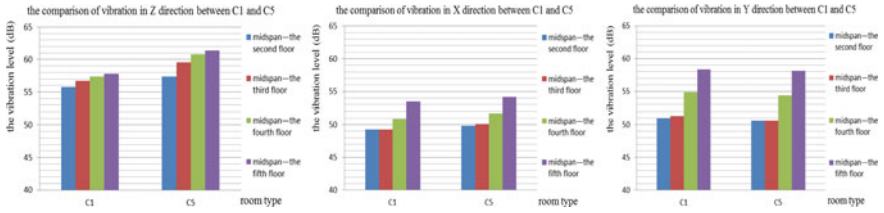

Fig. 16 Comparison of vibration level in the three directions in the mid-span of the floor with story height between Kitchen 1 and Kitchen 5

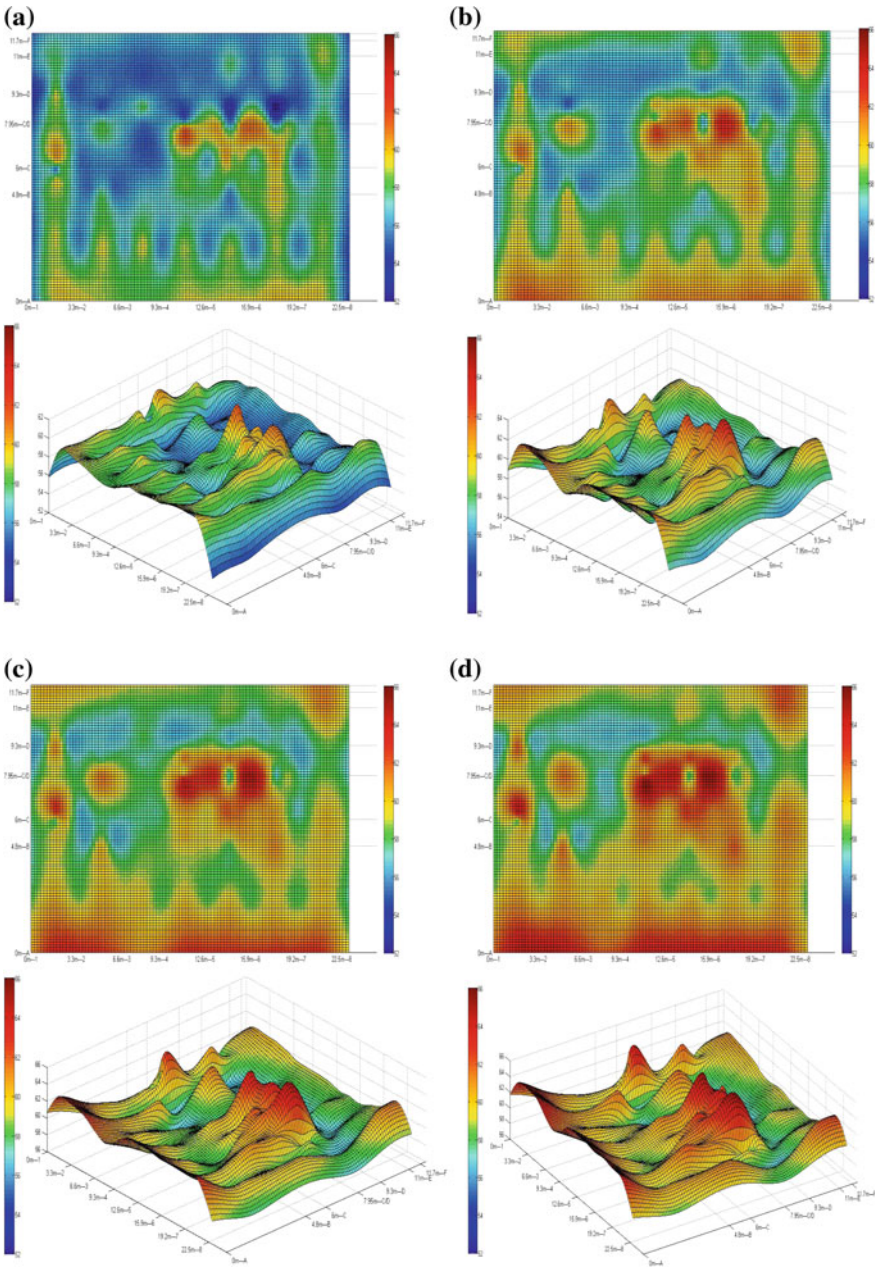

Fig. 17 Three-dimensional images of vertical vibration at all rooms on each floor: **a** the second floor, **b** the third floor, **c** the fourth floor, **d** the fifth floor

5.2 *Distribution Regularity of Vibration Response on the Same Floor*

The analysis of the existing structure is limited to the vibration in several rooms. The detailed description of the vibration situation in each room was not described. The 3D cloud image displays the vibration situation in each room, and Fig. 17 indicates the vibration strength distribution in each room on every floor when the subway passes by the building, which can provide a basis for macro-comparison.

Figure 17 shows the three-dimensional cloud result based on the numerical analysis in Sect. 5.1. In addition, it shows that vibration intensity has relationships with certain parameters, such as room depth and room width, slab properties, and floor location. The three-dimensional images facilitate visual qualitative analysis of the train-induced vibration and provide a strong basis for the environmental assessment of the existing structures and their subsequent isolation analysis [15].

6 Conclusion

1. When the subway passes, the vertical vibration level in the center of the large span indoor floor slab is 1–3 dB larger than that in the wall–floor junction, and the vertical vibration level in the center of the small span floor slab is 0.3–2 dB larger than that in the wall–floor junction.
2. The cheap precast slab has a greater amplification effect of vertical vibration than that of the cast in situ floor slab. The vibration intensity in precast slab ash seam position compared with that of the precast slab without mortar joint processing is higher by approximately 2–3 dB, and the vibration strength amplification between the precast ash seam slab is visible.
3. (a) The influence of room depth on vibration strength is small and negligible; (b) the influence of room width on vertical vibration is high. Greater room width results in higher vibration intensity.
4. Vibration intensity has relationships with certain parameters, such as room depth and room width, slab properties, and floor location.

Acknowledgements This work is supported by the National Natural Science Fund (51708450), Basic Research Project of Natural Science in Shaanxi Province (2018JQ5169), Ph.D. Research Start-Up Project (107-451115002), and School-Level Scientific Research Project (2016CX025).

References

1. Zhang N, Xia H, Yang WG et al (2011) Prediction and control of building vibration under metro excitations. In: Proceedings of the 8th international conference on structural dynamics (EURODYN 2011), Leuven, Belgium, pp 705–711
2. Banlendra T, Chua H, Lo KW et al (1989) Steady-state vibration of subway-soil-building system. J Eng Mech 115(1):145–162
3. Chua KH, Lo KW et al (1995) Building response due to subway train traffic. J Geotech Eng 121(11):747–754
4. Gupta S, Liu WF, Degrande G et al (2008) Prediction of vibrations induced by underground railway traffic in Beijing. J Sound Vib 310(3):608–630
5. Ding DY, Gupta S, Liu WN et al (2010) Prediction of vibrations induced by trains on line 8 of Beijing metro. J Zhejiang Univ Sci A 11(4):208–293
6. Erkal A, Laefer D, Fanning P, Durukal E, Hancilar U, Kaya Y (2010) Investigation of the rail-induced vibrations on a masonry historical building. In: 7th international conference on structural analysis of historic constructions: strengthening and retrofitting
7. Breccolotti M, Materazzi AL, Salciarini D et al (2011) Vibrations induced by the new underground railway line in Palermo, Italy—experimental measurements and FE modeling. In: Proceedings of the 8th international conference on structural dynamics (EURODYN 2011), Leuven, Belgium, pp 719–726
8. Development Planning Committee of Shaanxi Province (2002) Code for acceptance of constructional quality of masonry engineering (GB 50203-2002). China Architecture & Building Press, Beijing
9. Ministry of Construction of the People's Republic of China (2001) Unified standard for reliability design of building structures (GB 50068-2001). China Architecture & Building Press, Beijing
10. Ministry of Construction of the People's Republic of China (2002) Code for design of concrete structures (GB 50010-2002). China Architecture & Building Press, Beijing
11. Chopra AK (2005) Dynamics of structures: theory and applications earthquake engineering (trans: Xie L). Higher Education Press, Beijing
12. Wang TY (2007) Metro train-induced vibrations and study on the isolation method of buildings. College of Civil Engineering, Tongji University
13. Hanazato T, Ugai K, Mori M et al (1991) Three-dimensional analysis of traffic-induced ground vibrations. J Geotech Eng 117(8):1133–1151
14. Chua KH, Lo KW, Balendra T (1995) Building response due to subway train traffic. J Geotech Eng 121(11):747–754
15. Xia Q, Qu WJ (2017) Experimental and numerical studies of metro train-induced vibrations on adjacent masonry buildings. Int J Struct Stab Dyn 16(10):1550067–1550094
16. Xia Q, Qu WJ (2014) Numerical analysis on metro train-induced vibrations and their influences and affecting factors on existing masonry building. J Vib Shock 33(6):189–200